# Prediction of Surface Treatment Effects on the Tribological Performance of Tool Steels Using Artificial Neural Networks

**Liborio Cavaleri [1], Panagiotis G. Asteris [2],[\*] , Pandora P. Psyllaki [3], Maria G. Douvika [2], Athanasia D. Skentou [2] and Nikolaos M. Vaxevanidis [4]**

[1] Department of Civil, Environmental, Aerospace and Materials Engineering (DICAM), University of Palermo, Viale delle Scienze, 90128 Palermo, Italy

[2] Computational Mechanics Laboratory, School of Pedagogical and Technological Education, Heraklion, GR 14121 Athens, Greece

[3] Department of Mechanical Engineering, University of West Attica, 12244 Egaleo, Greece

[4] Laboratory of Manufacturing Processes and Machine Tools (LMProMaT), Department of Mechanical Engineering Educators, School of Pedagogical and Technological Education (ASPETE), ASPETE Campus, N. Heraklion, GR 14121 Athens, Greece

[\*] Correspondence: panagiotisasteris@gmail.com; Tel.: +30-210-2896-922

check for updates

**Abstract:** The present paper discussed the development of a reliable and robust artificial neural network (ANN) capable of predicting the tribological performance of three highly alloyed tool steel grades. Experimental results were obtained by performing plane-contact sliding tests under non-lubrication conditions on a pin-on-disk tribometer. The specimens were tested both in untreated state with different hardening levels, and after surface treatment of nitrocarburizing. We concluded that wear maps via ANN modeling were a user-friendly approach for the presentation of wear-related information, since they easily permitted the determination of areas under steady-state wear that were appropriate for use. Furthermore, the achieved optimum ANN model seemed to be a simple and helpful design/educational tool, which could assist both in educational seminars, as well as in the interpretation of the surface treatment effects on the tribological performance of tool steels.

**Keywords:** artificial intelligence techniques; artificial neural networks; soft computing techniques; tribological performance

## 1. Introduction

Mechanical systems commonly incorporate assemblies characterized by the contact of solid components moving relevant to each other, in order to transfer motion, power, or mechanical loading. These coupled components constitute what is known as a tribosystem or a tribopair, which is defined by the construction materials and geometry of the solids, with its operating parameters being the applied load, the relevant speed, and the environmental conditions (i.e., lubrication, temperature, humidity). In the case of malfunction of such assemblies, the operation of the entire mechanical system is jeopardized. For example, typical assemblies on a vehicle include:

- The brakes, where a consumable brake pad, through the application of a force, slides against the disc brake to suspend the wheel motion [1].
- The clutch assembly, where the clutch disk slides against the pressure plate to disengage power to the drive train, enabling the vehicle to stop, start, or shift gears [2].

- The air conditioning assembly, where the pulley directly attached to the compressor is coupled to the engine crankshaft via two tensioner pulleys and a polymer V-belt. Poor operation of any of the pulleys would result in stoppage of the belt motion, eventually leading to the interruption of the electrical control circuit.

During the operation of a tribosystem, wear of the two solids in contact and the progressive loss of material from the conjugated surfaces is expected. Hence, for the construction of such mechanical assemblies, a designer should select materials that will ensure steady-state operation, uniform and progressive wear, and a known rate of material loss. In the case of metallic components, wear takes place via the adhesive mechanism [3], which promotes microscopic plastic shearing of the asperities in touch and material transfer between the two surfaces. However, in several cases, the malfunction of metallic tribosystems can be attributed to different failure causes, such as galling [4], cracking, extensive oxidation, or severe plastic deformation [5], which are associated with improper materials selection for the given application. Galling is understood as the instantaneous increase of the friction coefficient (i.e., sudden difficulty in motion), whilst the operating parameters have not been altered. This, in combination with simultaneous tearing, significant plastic deformation, and massive material transfer constitutes a disastrous adhesive wear mechanism that could result in seizure—virtual welding of the two surfaces—eventually rendering the relevant motion of the two metallic bodies impossible.

In the field of metal working, extrusion/casting/forging dies, blades for hot shearing, and hot extrusion tools are typical examples of heavily loaded tribosystems, that are prone to any of the above failure modes. For such applications, it is recommended to use highly-alloyed steels, known as tool steels. These tool steels are special steel grades, usually incorporating a significant number of carbide-forming elements. Depending on their specific chemical composition, tool steels exhibit an interesting combination of properties, such as high toughness, shock resistance, machinability, abrasion, and heat resistance. In particular, their high hardenability and dimensional stability allow their heat treatment, resulting in materials that are within a wide range of bulk hardness values. All of the steels are available from manufacturers in their soft-annealed state (22–24 HRC), and they are subjected to further heat treatments to acquire the bulk hardness level required depending on the mechanical loading they are going to bear during service. In general, the heat treatment follows thermal cycles that include preheating, austenitization, and three successive tempering stages; where the specific relevant procedure is described in detail in the available literature [6].

Furthermore, metallic components that are designed to participate in tribosystems often require additional surface modification to enhance their fatigue, wear, and corrosion resistance. For example, the enhancement of surface properties is required in the case of tool steel molds that are used for the injection or compression of plastics. In the past, several non-conventional techniques based on the use of high energy beams [7–9] have been proposed for the surface treatment of Fe-alloys, with very promising scientific results. Nevertheless, owing to their relative lower installation and operational costs, thermochemical surface treatments, such as nitriding and nitrocarburizing, still remain the industrial-level surface treatments of choice for steels and cast irons [10]. Compared to other nitrocarburizing techniques [11–14], Tufftriding, despite the drawback of a necessary post-processing waste treatment step [15], is the most widespread, since it is less expensive, conceptually simpler, and provides highly reproducible results. It involves the treatment of metallic components in molten cyanide salt baths at 580 °C [16], a temperature lower than the eutectoid point (591 °C) of the Fe–N phase diagram, thereby allowing the simultaneous diffusion of nitrogen and carbon atoms into the ferrite lattice [6]. This results in the formation of two distinct surface layers of different nitrogen concentration. The layer on the top of the treated surface is known as the compound or white layer, and it primarily consists of $\varepsilon$-carbonitride $Fe_{2-3}(C,N)$. The layer underneath is known as the diffusion zone and it is mainly composed of a $\alpha$-$(Fe,N)$ solid solution [17,18]. These two successive layers constitute the nitrocarburized case that can extend to a depth of several—tens up to hundreds of— micrometers.

Liquid nitrocarburizing is applied as the final chemical-heat treatment for the improvement of tribological performance of various machine parts and friction elements, which are subjected

to sliding or rolling friction. Research efforts aim to optimize the material selection and surface treatment parameters, considering the specific application demands. In this context, the performance of nitrocarburized steels has been assessed under sliding [5,19,20], rolling [12], erosion [21], and/or corrosion [22] conditions.

Despite the fact that extended experimental research on these materials can be found in the international literature, a reliable quantitative tool, that is able to predict the tool steels performance in plane-contact dry sliding tribopairs, is still missing. The strongly nonlinear dependence of the friction and wear coefficients on parameters, such as the applied pressure, the rotational speed, and the bulk hardness (HRC), render the development of an analytical formula for the prediction of tribological performance, using deterministic methods, a rather difficult issue.

Meanwhile, artificial neural networks (ANNs) have emerged over the last decades as an attractive meta-modelling technique that is applicable to a vast number of scientific fields, including material science. An important characteristic of ANNs is that they can be used to build soft-sensors, i.e., models with the ability to estimate critical quantities without having to measure them [23]. In particular, such surrogate models can be constructed through a training process with only a few available data that can be used to predict pre-selected model parameters, reducing the need for time- and cost-consuming experiments. Thus far, the literature includes studies in which soft computing techniques, such as ANNs, were implemented for predicting the mechanical properties and behavior of materials. It should be stated that in the scientific field of engineering, the use of soft computing techniques has proven to be the salient meta-computing approach that contributes in a reliable and robust manner in cases where deterministic methods have failed [24–29]. Useful and detailed state-of-the-art reports can be found in the published research works of Ripley [30] and Adeli [31].

The primary aim of this work was to develop an ANN model to predict the performance of three steel grades in plane-contact dry sliding tribopairs. In particular, for the development and training of NN models, a large database consisting of 216 datasets was composed, based on the experimental results of 216 steel cylindrical specimens tested under non-lubricating sliding friction conditions, to support the research presented herein. Specifically, nine parameters characterized each specimen. In particular, the first three parameters encoded the type of materials, the next two parameters defined whether the material was nitrocarburized or not, and the next three parameters were the values of the applied pressure, the rotational speed, and the bulk hardness (HRC). The last parameter corresponds to whether the material exhibits uniform wear; where the ability to predict uniform–or not–wear during operation of the assemblies is highly important and desirable. The first eight parameters were used as input parameters, whilst the last one was selected as the output parameter. The optimum developed NN model proved to be very successful, exhibiting highly reliable predictions. Using the proposed optimum NN model, we produced a set of "tribological performance" maps for each one of the three steel grades, determining the areas of recommended and non-recommended use.

## 2. Short Literature Review

Several studies have addressed the issue of applying ANN techniques to predict the tribological performance of tribopairs. As early as 1996, ANNs were first introduced to assist in this issue, when Rutherford et al. [32] applied the technique to analyze the hardness and abrasive wear resistance of TiN/NbN PVD-deposited multilayers, and correlated them to the specific composition of the thin films. Jones et al. [33] showed the feasibility of using neural networks to predict life data for different material/mechanical systems (rub shoe, pin-on-disk, and four-ball rigs), via the proper selection of input variables that influenced the tribological behavior of each particular system. Ramesh and Gnanamoorthy [34] used ANNs to describe the friction and wear behavior of various surface-treated structural steels fretted against bearing steel. The surface treatment applied comprised liquid nitriding, boriding, as well as MoS2 spraying, whilst 35 pairs of friction and wear experimental datasets were used to develop the ANN. Similarly, the wear mechanisms of glass fiber reinforced epoxy were investigated via pin-on-roller tests against hardened steel and the experimental data were used to

identify the areas of mild, severe, and ultra-severe wear on a "normalized force"-"normalized velocity" chart produced with the aid of neural networking algorithms [35]. More recently, several works have emerged on the use of ANNs for the prediction of the wear of composite metallic matrix materials, based on the combined experimental investigation of the weight losses during pin-on-disk sliding and the percentage of the reinforcing constituent of the material [36–39]. Abdelbary et al. [39] developed an ANN architecture for modeling the wear of polyamide 66 during dry sliding, introducing the applied load, the load ratio, the number of surface cracks, the lubricant's thickness, and the linear wear rate of the material under study as input data. Stojanovic et al. [40] combined the Taguchi method and ANN to optimize the percentage of particulate reinforcement of 2024 aluminum alloys that could ensure a minimum wear rate during dry sliding block-on-disc tests. The experimental data were used to develop a multiple linear regression model and an ANN model, where the latter proved to be more efficient. In 2018, Pillai et al. [41], focusing on the effects of prior heat treatment on the tribological performance of AISI A8 cold working tool steel, developed wear mechanism maps by applying K means clustering and neural networks. Detailed and in-depth state-of-the-art works can be found in References [41–48].

## 3. Need for Research

As already mentioned, due to the absence of an analytical model able to predict the tribological performance of metals and alloys, the selection of the material grade and its hardening level is performed in a rather empirical manner. The motivation for the work presented herein was to investigate the possibility of developing a reliable model that could predict the tribological performance of materials exhibiting elastoplastic behavior, considering crucial material characteristics, such as the grade and hardening level, as well as operational parameters, such as the applied pressure and rotational speed. Such a quantitative tool may lead to "tribological performance maps" that are relevant and tailored to the requirements of each particular application, thereby assisting in the selection of: (a) Materials for the manufacture of mechanical components that are designed to operate as parts of a tribo-system; (b) Appropriate heat treatment, aimed at materials hardening; and (c) Appropriate surface treatment to further expand a component's service life.

## 4. Artificial Neural Networks

### 4.1. General

Artificial neural networks (ANNs), which are a well-known artificial intelligence technique, have the ability to process and explore complex information (data) to solve classification and regression problems. The main advantage of an ANN is that it is capable of producing more reliable outcomes than conventional numerical analysis methods, as ANNs can handle complex problems with many input parameters, which would otherwise be very difficult to solve using traditional approaches [49–55].

The basic structure of an ANN is the artificial neuron, that is, a mathematical model which resembles the behavior of the biological neuron (Figure 1), but with a plethora of activation functions enabling the biological neuron's sigmoid activation function. To be precise, it should be noted that scientists have decoded only a small amount of the biological neural networks (BNNs) structure, behavior, and functions. Therefore, to be exact, the similarity between biological and artificial neural networks is mainly the morphological characteristics.
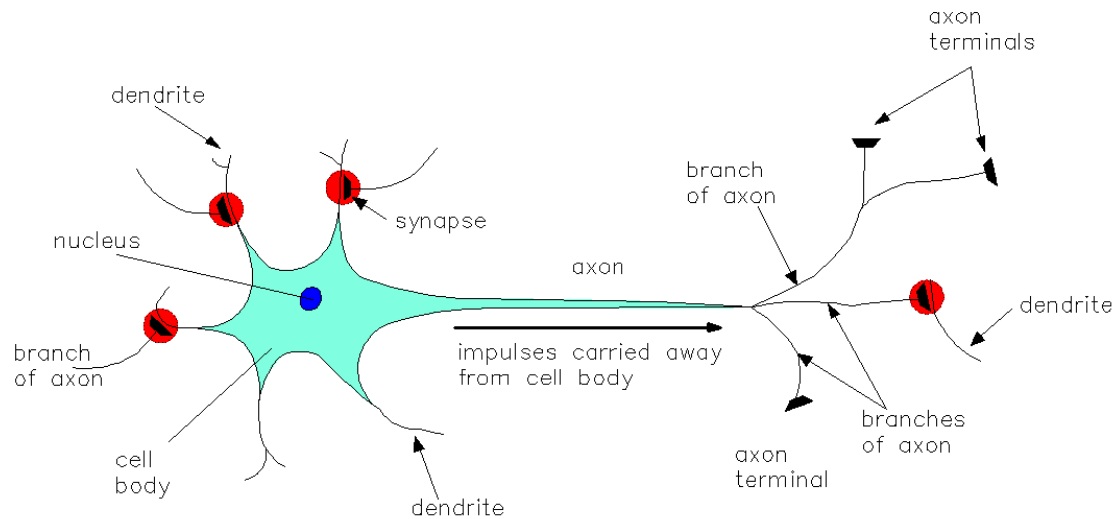
**Figure 1.** Schematic representation of biological neuron structure.

The structure of an ANN consists of three main layers, including input layers, hidden layers, and output layers. Out of these layers, the hidden layers use the activation function to pass and process the information from the input layers to provide results in the output layers, using artificial neurons (nodes). To train the ANN, there are several steps that need to be considered as follows: (i) select the architecture of the ANN which describes the way the artificial neurons are organized and linked; (ii) select the suitable activation function to be used in the hidden layers to learn the data; and (iii) select the loss function, metrics, which are used to update the weights of input parameters. Training the ANN can be considered as a function minimization problem, whereas the loss function (error function) is used to determine the optimum value of weights assigned for parameters used in the input layers. Different types of ANNs can be built using various optimization algorithms. In this study, we used the back-propagation neural network (BPNN), which is an effective optimization algorithm to train the ANN.

*4.2. Structure of the BPNN*

Known as a feed-forward, multilayer neural network, the BPNN does not have feedback loops. Thus, information passes on from the input layers towards the output layers, and the neurons of the same layer are connected with all the neurons of the subsequent and previous layer; however, not connected to one another. The standard structure of a BPNN can be presented as follows:

$$N - H_1 - H_2 - \ldots - H_{NHL} - M \tag{1}$$

where M is defined as the number of output parameters (output neurons), N is defined as the number of input parameters (input neurons); $H_i$ corresponds to the number of neurons in the i-th hidden layer (i = 1, . . . ,NHL); and NHL is known as the number of hidden layers.

Despite the fact that the majority of researchers dealing with ANN techniques use multilayer NN models, mathematical ANN models with only one hidden layer can serve as reliable computational tools for certain forecast problems.

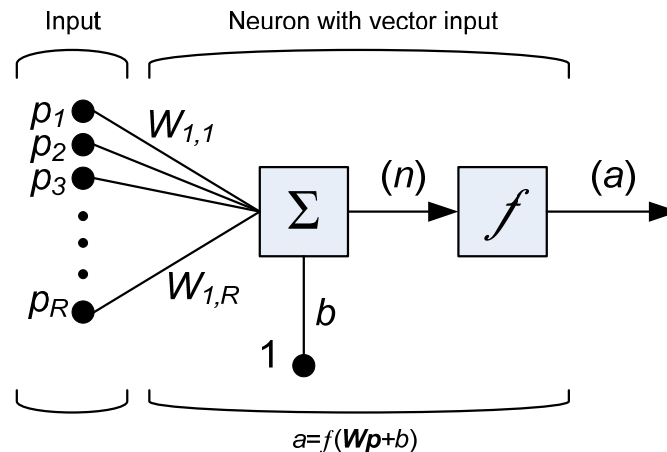Figure 2 depicts the structure of a single node (with the corresponding R-element input vector) of a hidden layer.

**Figure 2.** Architecture of a neuron with a single R-element input vector.

Consider each neuron i, the weights $w_{i,1}, \ldots, w_{i,R}$ are used to multiply with the individual element inputs $p_1, \ldots, p_R$, and the weighted values are then put into the junction of the summation function, of which the input vector $p = [p_1, \ldots, p_R]^T$ and the dot product $(W{\cdot}p)$ of the weight vector $W = [w_{i,1}, \ldots, w_{i,R}]$ are generated. Presented below is the argument of the transfer function $f$, where the threshold b (bias) is added to the dot-product forming the net input n:

$$n = W{\cdot}p = w_{i,1}p_1 + w_{i,2}p_2 + \ldots + w_{i,R}p_R + b, \tag{2}$$

The complexity and performance of an ANN might be influenced by the selection of the activation function $f$. There are different activation functions used to train an ANN, such as sigmoidal transfer functions, the logistic sigmoid, and the hyperbolic tangent transfer functions [56–59]. In this study, we found that the logistic sigmoid and the hyperbolic tangent transfer functions were appropriate activation functions for the problem under examination. Using the activation functions, the training data were input to the network, which attempted to transfer the information from the input layers to the output layers. During this process, the weights were adjusted to minimize the loss function, presented as follows:

$$E = \sum (x_i - y_i)^2, \tag{3}$$

where $x_i$ and $y_i$ are defined as the true value (ground truth) and the predicted value, respectively, of the i-th dataset.

## 5. Materials and Methods

A prerequisite for the successful function of artificial neuron networks is the use of an extended and reliable database that is capable of training the system. The extent of the experimental database should be large enough to provide the necessary amount of input information, and, at the same time, restricted enough to avoid overuse of costly experimental resources. The optimization of the ANNs proposed for the prediction of the tribological performance of tool steels, is based on the experimental datasets presented briefly below.

### 5.1. Experimental Procedures—Database

The reliability of a developed artificial network is directly dependent on the reliability of the database compiled and utilized in its design and training. In particular, to develop a reliable neural network, a reliable database is necessary, and one which incorporates datasets covering a wide range of possible values of the input parameters involved. Thus, in the current study, an adequate amount of reliable experimental data was necessary, i.e., data which could describe the tribological performance of tool steels in a satisfactory manner. It should be noted that a high number of datasets does not necessarily

lead to the development of a more accurate ANN. For example, datasets which refer to similar values of the parameters, without covering a wide range of possible values, cannot assist in describing and revealing the material's behavior in relation to the input parameters. A database incorporating data which describes the influence of all parameters on the output parameter is necessary, and the database should incorporate the whole range of possible values of input parameters. Furthermore, the accuracy of the data incorporated in the database is of high importance, because if erroneous values are introduced into the training datasets, the artificial neural network will be trained using these values and will provide erroneous prediction values. This is indicative of the meaning of the famous expression in informatics "garbage in garbage out" (GIGO).

Multitudinous experimental tests were conducted to support the work presented herein. Three different steel grades, two of them intended for cold working and the third for hot working applications, were chosen as model materials. Table 1 shows their AISI (American Iron and Steel Institute) classifications. Each grade was properly heat-treated to achieve three series of specimens per grade, presenting a bulk hardness of 40, 50, and 60 HRC. After hardening, half of the specimens of each series were further subjected to liquid nitrocarburizing via the Tufftriding technique as described in Reference [16]. Finally, all steel grades, with hardening treatment, as well as with both hardening and surface treatment, were subjected to plane-contact dry sliding, under the common testing conditions described below.

**Table 1.** Characteristics of the materials employed in the present study.

| Material Examined | AISI Classification | Application |
|---|---|---|
| Steel A | D2 | Cold working tools |
| Steel B | - | Cold working tools |
| Steel C | H13 | Hot working tools |

A Cameron–Plint® pin-on-disk tribometer, equipped with a force transducer was used for the real-time recording of the sliding friction coefficient evolution. During all tests, two identical cylindrical pins (Ø 8 mm, 55 mm length) of the steel grade under examination were mounted and pressed against a rotating disk (counterbody), manufactured from AISI D6 steel and heat-treated to a bulk hardness of 62 HRC. Figure 3 depicts a schematic representation of the testing rig operation. Detailed and in-depth descriptions can be found in the authors' recently published work [60].
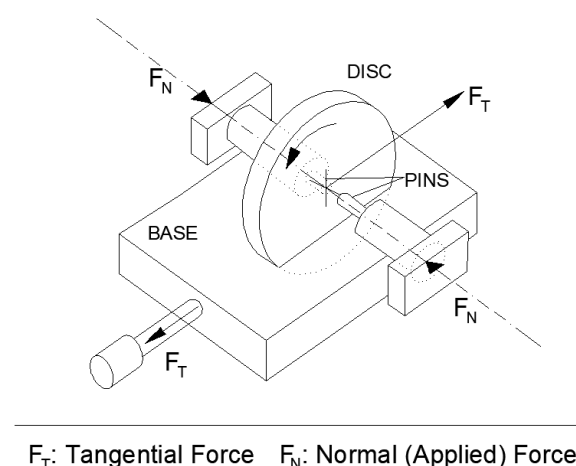


$F_T$: Tangential Force　　$F_N$: Normal (Applied) Force

**Figure 3.** Schematic representation of the Cameron-Plint® pin-on-disk testing tribometer.

All sets of specimens were tested by applying pressures of 0.3, 0.5, and 0.7 MPa, as well as rotational speed values of 300 and 1050 rpm. The experiments were carried out at ambient atmosphere (25 °C, 50% RH) and lasted for 25,000 revolutions, except for cases where galling occurred, leading to test interruption. The worn surfaces were post-observed at low magnification via an optical

stereoscope to clarify the different types of materials degradation during plane-contact sliding, even in cases where galling did not take place. Finally, the outcome of all series of experiments allowed the distinguishing of four different wear/failure types of the operating tribosystems, i.e., one desirable and three non-desirable, as summarized in Table 2. More detailed analyses on these evaluation criteria, including friction coefficient evolution diagrams and stereoscopic images, were reported in a previous work [60]. Based on the above, we prepared a database consisting of 216 datasets, corresponding to 72 datasets for each steel grade tested. The compiled database is presented in the excel file titled "Database" in Supplementary Materials.

**Table 2.** Wear/failure modes used as evaluation criteria for the performance of the tribosystems examined.

| Wear/Failure Type | Characteristics | Performance of the Tribosystem |
|---|---|---|
| Mode I | Uniform and progressive material loss | Desirable behavior during service |
| Mode II | Galling observed as a sudden increase of the friction coefficient | Non-desirable, due to the incipient interruption of the tribosystem operation |
| Mode III | Plastic flow of the material at the vicinity of the contact, in some cases accompanied by local oxidation | Non-desirable material behavior during application |
| Mode IV | Severe plastic deformation that can be macroscopically observed | Non-desirable material behavior due to the distortion of the mechanical parts |

*5.2. Material Encoding*

During the development process of the BPNN model, emphasis was placed on the encoding of the experimental data. These data involved measurements from five different cases, i.e., three different steel grades with and without post-hardening surface treatment. To simulate the crucial characteristics of the materials, we used five encoding parameters (i.e., the five shown in Table 3, as well as in columns 4–8 in the excel file titled "Database" in Supplementary Materials. Furthermore, the output parameter was encoded: 0 for desirable performance (Mode I, Table 2) and 1 for non-desirable (Modes II, III, and IV, Table 2). This encoding protocol has been successfully applied in the previous works of some of the present authors, addressing the issue of electro-discharge machining using ANNs [56,57]. Based on the above, Table 4 presents the input and output parameters, as well as their values.

**Table 3.** Materials encoding.

| Case | Material | Treatment | Encoding Parameters | | | | |
|---|---|---|---|---|---|---|---|
| | | | Material | | | Treatment | |
| I | Steel A | H.T. [1] | 1 | 0 | 0 | 1 | 0 |
| II | | H.T. + S.T.[2] | | | | 0 | 1 |
| III | Steel B | H.T. | 0 | 1 | 0 | 1 | 0 |
| IV | | H.T. + S.T. | | | | 0 | 1 |
| V | Steel C | H.T. | 0 | 0 | 1 | 1 | 0 |
| VI | | H.T. + S.T. | | | | 0 | 1 |

[1] Heat treatment aiming to bulk hardening. [2] Surface treatment (nitrocarburizing) after heat treatment.

**Table 4.** The input and output parameters used in the development of back-propagation neural networks (BPNNs).

| Parameters | | Units | Type | Value |
|---|---|---|---|---|
| No. | Variable | | | |
| 1 | Material Encoding Parameter 1 | - | Input | 0 or 1 |
| 2 | Material Encoding Parameter 2 | - | Input | 0 or 1 |
| 3 | Material Encoding Parameter 3 | - | Input | 0 or 1 |
| 4 | Material Encoding Parameter 4 | - | Input | 0 or 1 |
| 5 | Material Encoding Parameter 5 | - | Input | 0 or 1 |
| 6 | Bulk Hardness (BH) | HRC | Input | 40, 50 and 60 |
| 7 | Rotational Speed (RS) | rpm | Input | 0, 300 and 1050 |
| 8 | Applied Pressure (AP) | bar | Input | 0, 3, 5 and 7 |
| 9 | Tribological Performance | - | Output | 0 or 1 |

### 5.3. Training Algorithms

Training the BPNN models is the most important step in developing the optimal artificial neural network. Each problem is best expressed with the use of a specific training function. For this purpose, in the current research, we explored a wide variety of training functions to select the most appropriate function that could provide the ANN with the highest accuracy in terms of prediction capability. We employed and assessed the quasi-Newton, resilient, one-step secant, gradient descent with momentum and adaptive learning rate, and Levenberg–Marquardt back propagation algorithms. The Levenberg–Marquardt training function provided, by far, the best results, achieving prediction with the highest accuracy [61]. This algorithm appeared to present the best results in non-linear problems, whilst at the same time, it appeared to be the least time consuming method to train moderate-sized feedforward neural networks (meaning networks with up to several hundred weights). The fact that the solution of the Levenberg–Marquardt matrix equation was a built-in function of the MATLAB® software was an added benefit and advantage to its selection. This enhanced the efficiency of its use.

### 5.4. Normalization of Data

To enhance the accuracy and efficiency of the developed ANN, normalization of the data (a frequently encountered issue in the field of soft computing techniques pre-processing stage) was decided. Specifically, we employed the Min-Max [62] normalization method for the eight input parameters, as stated in Table 4, and the single output parameter. To this aim, it was important to normalize the data within a defined range of appropriate upper and lower limit values, especially considering the fact that the selection of the appropriate limit values could have a highly beneficial effect on the ANNs' learning rate, as presented by Iruansi [63,64]. In the present study, the input parameters, as well as the output parameters, were normalized in the range of values [0.10, 0.90].

### 5.5. BPNN Model Development

Consequently, we developed and evaluated a high number of BPNN models. We used 108 data-points to train each ANN model, corresponding to 50% of the total number of data-points, whilst validation of the developed model was achieved through the use of 54 data-points, corresponding to 25% of the total data-points. The remaining 25% of the available data-points, amounting to 54 data-points, were used to test the trained ANN.

It was decided to investigate ANNs with hidden layers ranging from 1 to 2, whilst the number of neurons for each hidden layer ranged from 1 to 30. In addition to the aforementioned scenarios, we examined various activation functions for the development and training of each artificial neural network. In particular, we investigated the log-sigmoid transfer (logsig), the linear transfer (purelin), and the hyperbolic tangent sigmoid transfer (tansig) functions, to select the most appropriate function, capable of achieving optimal results [65–73].

Thus, the ANNs were trained by employing the parameters as stated in Table 5. To compare the results provided by the different ANNs, beforehand, the datasets were randomly divided into training datasets, validation datasets, and testing datasets. The grouping of the datasets was performed manually by the user prior to the training of the various ANNs, and indices were used to mark the group to which each dataset was attributed.

**Table 5.** Training parameters of BPNN models.

| Parameter | Value |
| --- | --- |
| Training Algorithm | Levenberg-Marquardt Algorithm |
| Normalization | Minmax in the range 0.10–0.90 |
| Number of Hidden Layers | 1; 2 |
| Number of Neurons per Hidden Layer | 1 to 30 by step 1 |
| Control random number generation | Rand (seed, generator) where generator ranges from 1 to 10 by step 1 |
| Training Goal | 0 |
| Epochs | 250 |
| Cost Function | MSE [1]; SSE [2] |
| Transfer Functions | Tansig (T) [3]; Logsig (L) [4]; Purelin (P) [5] |

[1] Mean Square Error. [2] Sum Square Error. [3] Hyperbolic tangent sigmoid transfer function. [4] Log-sigmoid transfer function. [5] Linear transfer function.

### 5.6. Mathematical Model Validation

The most crucial and challenging task after the training and development process of ANN models is the evaluation of their performance, as well their reliability. A number of statistical indices were calculated to assess the performance of the developed FF-ABC-NN model. In particular, we calculated the root mean square error (RMSE) and the mean absolute percentage error (MAPE), where lower calculated values correspond to higher predictive accuracy of the model, as well as the Pearson correlation coefficient $(R^2)$, where the higher the $R^2$ value, the better the fitting between experimental and predicted values. To the best of the authors' knowledge, the RMSE performance index seems to be the most accurate index for the evaluation and ranking of ANN mathematical models, for selection of the optimum and most robust model. Nevertheless, the majority of researchers use the Pearson correlation coefficient for the evaluation of ANN models, usually in conjunction with other performance indexes [74–78]. The statistical indices used in the present study were calculated using the following, well known and available in the literature, expressions [79–87]:

$$RMSE = \sqrt{\frac{1}{n} \sum_{i=1}^{n} (x_i - y_i)^2}, \tag{4}$$

$$MAPE = \frac{1}{n} \sum_{i=1}^{n} \left| \frac{x_i - y_i}{x_i} \right|, \tag{5}$$

$$R^2 = 1 - \left( \frac{\sum_{i=1}^{n} (x_i - y_i)^2}{\sum_{i=1}^{n} (x_i - \overline{x})^2} \right), \tag{6}$$

where $n$ denotes the total number of datasets, and $x_i$ and $y_i$ represent the predicted and target values, respectively.

## 6. Results and Discussion

Based on the above, we investigated a total of 982,800 different BPNN models to find the optimum NN model for the prediction of tribological performance of the experimentally tested tool steel grades. We also studied combinations of the use or non-use of the normalization technique and the use of one or two hidden layers.

The developed ANN models were sorted in a decreasing order according to their RMSE value. Based on this ranking, several reliable ANN architectures were found with a value of RMSE equal

to zero for all investigated cases (one or two hidden layers, with or without use of normalization technique). Amongst the most reliable mathematical models, it was important to select the simplest as the optimum BPNN model. Specifically, the 8-8-1 BPNN model was proposed as the optimum ANN for the prediction of the wear of the three tool steels. Its notation indicates that it corresponds to the case of one hidden layer with eight neurons (the minimum number of neurons), and without the use of any pre-processed normalization technique (Figure 4). As shown therein, the transfer functions are the log-sigmoid transfer function for the hidden layer and the hyperbolic tangent sigmoid transfer function for the output layer.
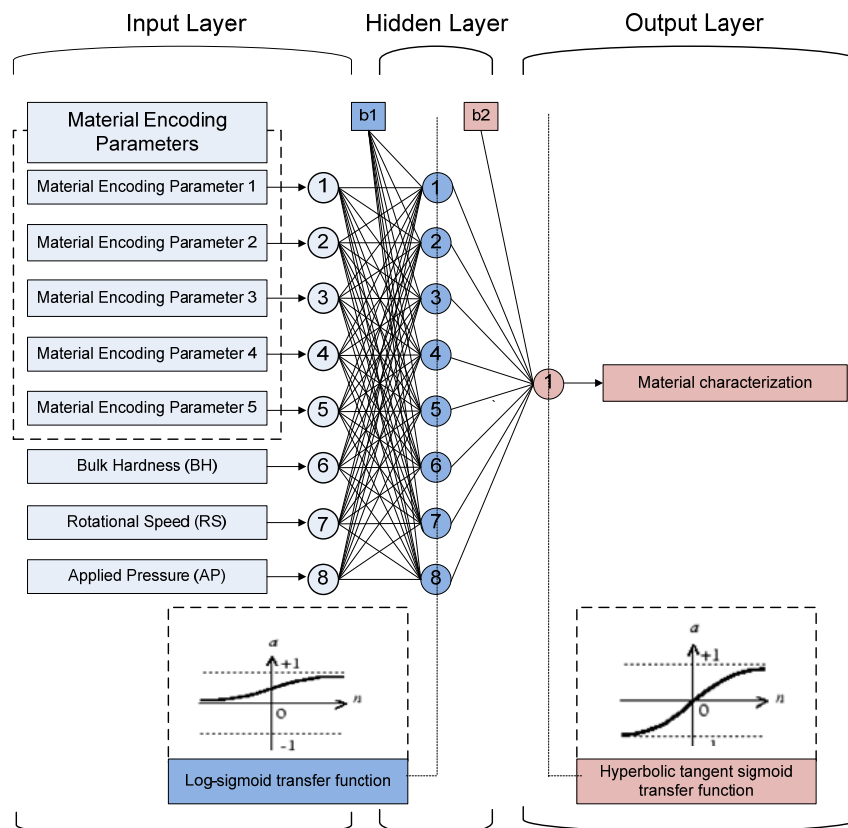


**Figure 4.** Architecture of the optimum 8-8-1 BPNN.

Using this proposed optimum ANN model, preliminary "safe operation area" maps of the tribological performance of the three steel grades were produced (Figures 5–7). These maps showed a material property on the *x*-axis, namely the bulk hardness, achieved by heat treatment, and an operational parameter during service on the *y*-axis, namely the applied pressure. Each map corresponded to one specific rotational speed and one surface state, either without or with the surface treatment of nitrocarburizing. In each figure, in addition to the experimentally tested rotational speed values of 300 and 1050 rpm, the predictions for an intermediate value of 600 rpm were also included.
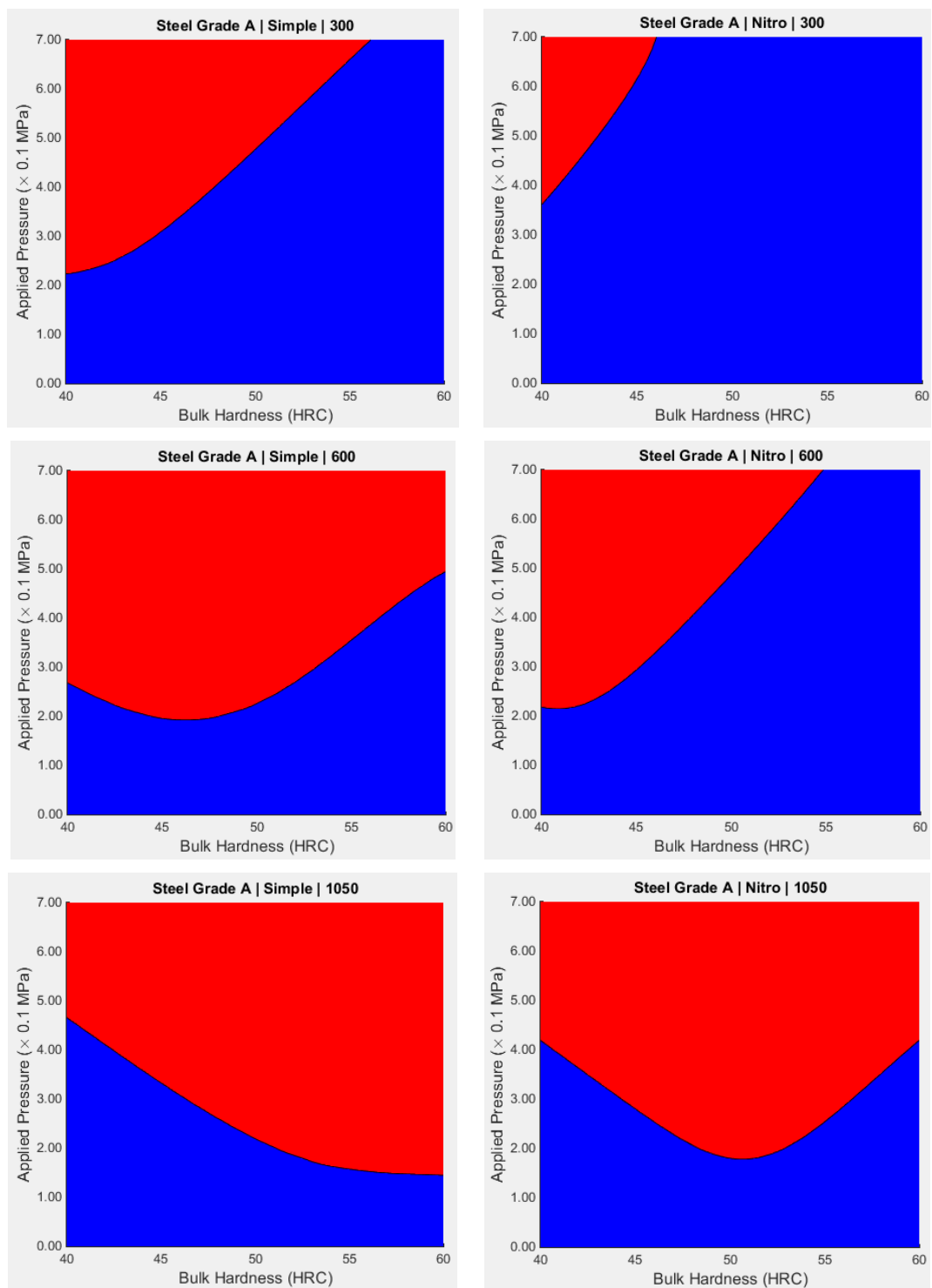
**Figure 5.** Maps of tribological performance for steel grade A, tested under three different rotational speeds 300, 600, and 1050 rpm: left column without surface treatment (before nitrocarburizing; right column after nitrocarburizing. The blue area corresponds to desirable uniform wear (Mode I), whilst the red one corresponds to non-desirable material behavior (Modes II, III, IV).
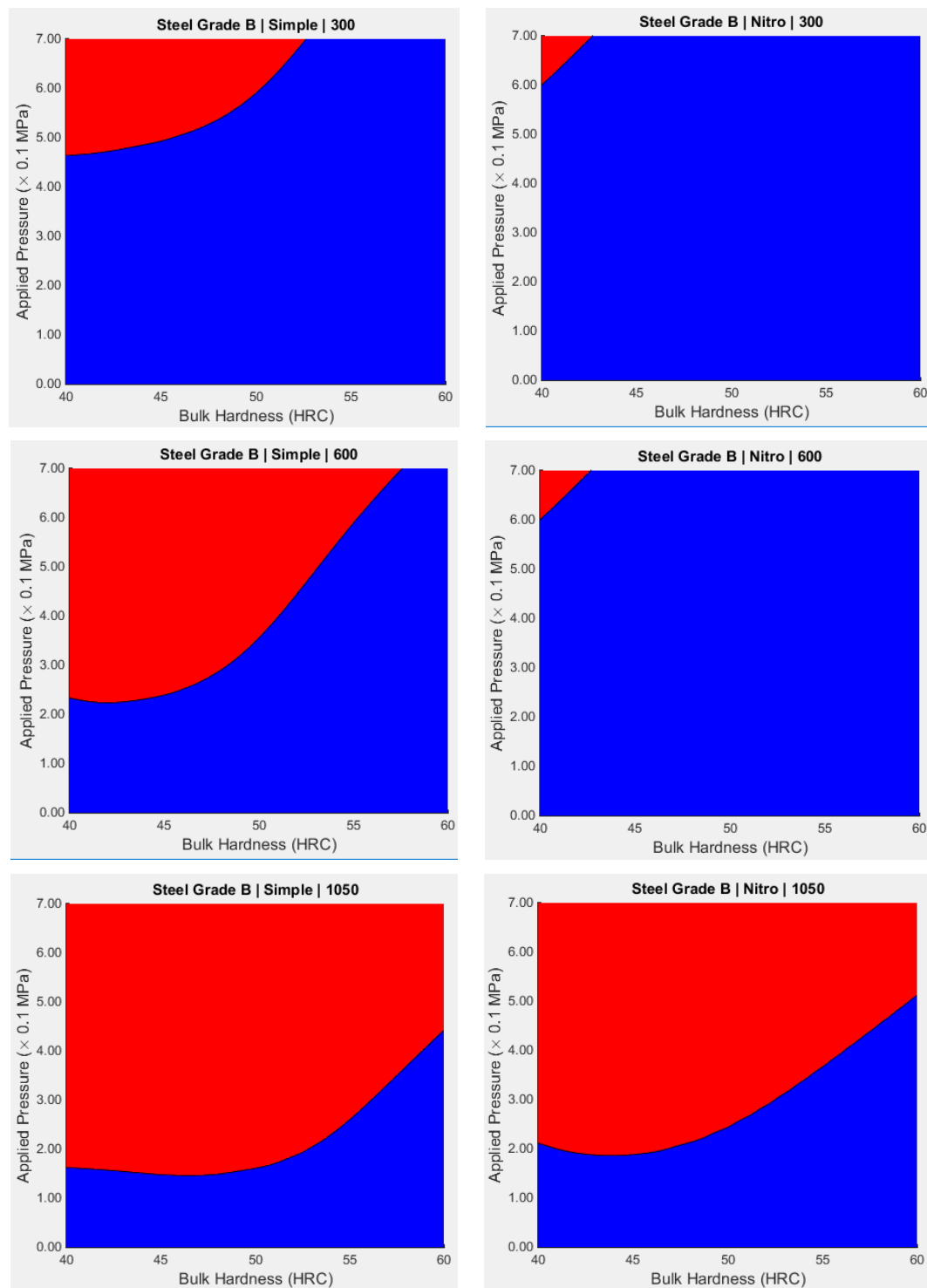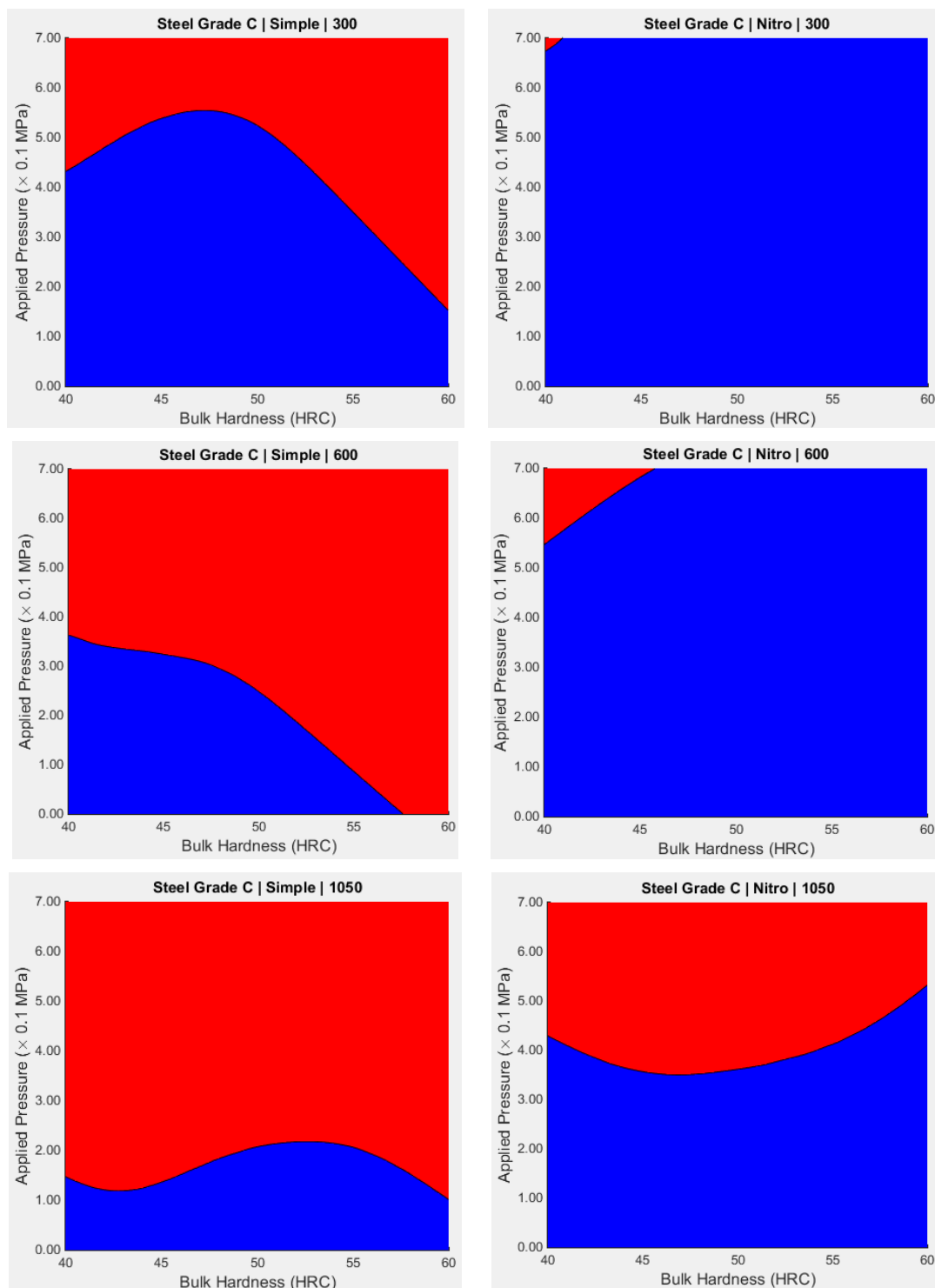
**Figure 6.** Maps of tribological performance for steel grade B, tested under three different rotational speeds 300, 600, and 1050 rpm: left column without surface treatment (before nitrocarburizing); right column after nitrocarburizing. The blue area corresponds to desirable uniform wear (Mode I), whilst the red one corresponds to non-desirable material behavior (Modes II, III, IV).

**Figure 7.** Maps of tribological performance for steel grade C, tested under three different rotational speeds 300, 600, and 1050 rpm: left column without surface treatment (before nitrocarburizing); right column after nitrocarburizing. The blue area corresponds to desirable uniform wear (Mode I), whilst the red one corresponds to non-desirable material behavior (Modes II, III, IV).

## 7. Limitations

It is worth noting that the application field of the proposed optimum neural system is defined within the range of parameter values used as input for its design and training. Specifically, the

proposed neural system provides reliable forecasts for parameter values ranging within the minimum and maximum value of the input parameters, as stated in Table 4.

The reliability of the neural system for parameter values beyond these limit values was quite restricted. It is also worth noting that, despite the satisfactory derived results, the proposed neural network should be applied with caution. Despite the fact that the database used was the largest set used in the relevant literature up to date, for the prediction of the surface treatment effects on the tribological performance of tool steels using ANNs, the authors considered that this database needs to be embellished with further experimental data. To this end, it is within the authors' plans to conduct further experiments related to these three metals. In particular, the experiments that are lacking are related to applied pressure equal to 2.00 bar, as well as experiments for rotational speed values of 600 and 900 rpm.

## 8. Conclusions

Wear maps for three different highly alloyed steel grades (two cold working steels and a hot working one) under a certain set of operating conditions were constructed by applying ANN modelling on an extended and reliable database of tribological experimental results.

Experimental results were obtained by performing plane-contact sliding tests under non-lubrication conditions on a pin-on-disk tribometer. The specimens were tested both in an untreated state, with different hardening levels, and after surface treatment of nitrocarburizing (Tufftriding technique).

From the numerous ANN models tested, the 8-8-1 BPNN model was selected as the optimum ANN for the prediction of the wear of the three tool steels; the transfer functions are the log-sigmoid transfer function for the hidden layer and the hyperbolic tangent sigmoid transfer function for the output layer.

From the application of the optimum ANN, the main results can be summarized as follows:

- Wear-related information can be easily presented in a comprehensive manner by the design of wear maps, as derived through the ANN modelling. Wear maps are user-friendly and allow the determination of areas under steady-state wear, which are recommended for use.
- When the operational parameters are evaluated as severe, it is recommended to select different steel grades.
- Higher values of bulk hardness correspond to a more extended steady-state wear region.
- Surface treatment by nitrocarburizing of the hardened steel has a beneficial effect, as it limits the region of non-recommended use.
- For a certain steel grade, the increase of the sliding speed decreases the region of recommended use.
- Nitrocarburizing seems to be more effective in the case of hot working steel grade than in the cases of cold working grades.

In addition, the proposed optimum ANN model seems to offer a simple design/educational tool, which can assist both for educational purposes, as well as the interpretation of the surface treatment effects on the tribological performance of tool steels.

## Abbreviations

AISI      American Iron and Steel Institute
ANNs      Artificial Neural Networks
BNNs      Biological Neural Networks
BPNNs     Back-Propagation Neural Networks
DNNs      Deep Neural Networks
HRC       Bulk Hardness
HT        Heat Treatment
logsig    Log-sigmoid transfer function
purelin   Linear transfer function
ST        Surface Treatment
tansig    Hyperbolic tangent Sigmoid transfer function

## References

1. Pantazopoulos, G.; Tsolakis, A.; Psyllaki, P.; Vazdirvanidis, A. Wear and degradation modes in selected vehicle tribosystems. *Tribol. Ind.* **2015**, *37*, 72–80.
2. Psyllaki, P.; Pantazopoulos, G.; Karaiskos, P. Failure mechanisms of an automobile clutch assembly cast iron pressure plate. *J. Fail. Anal. Prev.* **2012**, *12*, 16–23. [CrossRef]
3. Williams, J.A. *Engineering Tribology*; Oxford University Press: Oxford, UK, 1996.
4. Pantelis, D.I.; Pantazopoulos, G.; Antoniou, S.S. Wear behavior of anti-galling surface textured gray cast iron using pulsed-$CO_2$ laser treatment. *Wear* **1997**, *205*, 178–185. [CrossRef]
5. Psyllaki, P.; Kefalonikas, G.; Pantazopoulos, G.; Antoniou, S.; Sideris, J. Microstructure and tribological behaviour of liquid nitrocarburised tool steels. *Surf. Coat. Technol.* **2003**, *162*, 67–78. [CrossRef]
6. Karamboiki, C.-M.; Mourlas, A.; Psyllaki, P.; Sideris, J. Influence of microstructure on the sliding wear behavior of nitrocarburized tool steels. *Wear* **2013**, *303*, 560–568. [CrossRef]
7. Rodríguez, G.P.; de Damborenea, J.J.; Vàzquez, A.J. Surface hardening of steel in a solar furnace. *Surf. Coat. Technol.* **1997**, *92*, 165–170. [CrossRef]
8. Gemelli, E.; Gallerie, A.; Caillet, M. Improvement of resistance to oxidation by laser alloying on a tool steel. *Scr. Mater.* **1998**, *39*, 1345–1352. [CrossRef]
9. Katsamas, A.I.; Haidemenopoulos, G.N. Surface hardening of low-alloy 15CrNi6 steel by $CO_2$ laser beam. *Surf. Coat. Technol.* **1999**, *115*, 249–255. [CrossRef]
10. ASM Handbook. *Surface Engineering*; ASM International: Materials Park, OH, USA, 1996.
11. Zagonel, L.F.; Alvarez, F. Tool steel ion beam assisted nitrocarburization. *Mater. Sci. Eng. A* **2007**, *465*, 194–198. [CrossRef]
12. Corengia, P.; Walther, F.; Ybarra, G.; Sommadossi, S.; Corbari, R.; Broitman, E. Friction and rolling-sliding wear of DC-pulsed plasma nitrided AISI 410 martensitic stainless steel. *Wear* **2006**, *260*, 479–485. [CrossRef]
13. Mirjani, M.; Shafyei, A.; Ashrafizadeh, F. Plasma and gaseous nitrocarburizing of C60W steel for tribological applications. *Vacuum* **2009**, *83*, 1043–1048. [CrossRef]
14. Mirjani, M.; Mazrooei, J.; Karimzadeh, N.; Ashrafizadeh, F. Investigation of the effects of time and temperature of oxidation on corrosion behavior of plasma nitrided AISI 4140 steel. *Surf. Coat. Technol.* **2012**, *206*, 4389–4393. [CrossRef]
15. Pye, D. *Practical Nitriding and Ferritic Nitrocarburizing*; ASM International: Materials Park, OH, USA, 2003.
16. Pantazopoulos, G.A. Tufftriding and tennifer surface treatment. In *Encyclopedia of Tribology*; Wang, Q.J., Chung, Y.W., Eds.; Springer: Boston, MA, USA, 2013.

17. Yu, L. *Engineering Physical Metallurgy and Heat Treatment*; Mir Publishers: Moscow, Russia, 1977.

18. Torchane, L.; Bilger, P.; Dulcy, J.; Gantois, M. Control of iron nitride layers growth kinetics in the binary Fe-N system. *Metall. Mater. Trans. A* **1996**, *27*, 1823–1835. [CrossRef]

19. Pantazopoulos, G.; Papazoglou, T.; Psyllaki, P.; Sfantos, G.; Antoniou, S.; Papadimitriou, K.; Sideris, J. Sliding wear behaviour of a liquid nitrocarburised precipitation-hardening (PH) stainless steel. *Surf. Coat. Technol.* **2004**, *187*, 77–85. [CrossRef]

20. Pantazopoulos, G.; Psyllaki, P.; Kanakis, D.; Antoniou, S.; Papadimitriou, K.; Sideris, J. Tribological properties of a liquid nitrocarburised special purpose cold work tool steel. *Surf. Coat. Technol.* **2006**, *200*, 5889–5895. [CrossRef]

21. Dong, C.W. Erosion and wear behavior of nitrocarburized DC53 tool steel. *Wear* **2010**, *268*, 629–636.

22. Liu, R.L.; Yan, M.F. Improvement of wear and corrosion resistances of 17-4PH stainless steel by plasma nitrocarburizing. *Mater. Des.* **2010**, *31*, 2355–2359. [CrossRef]

23. Alexandridis, A. Evolving RBF neural networks for adaptive soft-sensor design. *Int. J. Neural Syst.* **2013**, *23*, 1350029. [CrossRef]

24. Armaghani, D.J.; Hajihassani, M.; Mohamad, E.T.; Marto, A.; Noorani, S.A. Blasting-induced flyrock and ground vibration prediction through an expert artificial neural network based on particle swarm optimization. *Arab. J. Geosci.* **2014**, *7*, 5383–5396. [CrossRef]

25. Armaghani, D.J.; Mohamad, E.T.; Narayanasamy, M.S.; Narita, N.; Yagiz, S. Development of hybrid intelligent models for predicting TBM penetration rate in hard rock condition. *Tunn. Undergr. Space Technol.* **2017**, *63*, 29–43. [CrossRef]

26. Pham, B.T.; Bui, D.T.; Pham, H.V.; Le, H.Q.; Prakash, I.; Dholakia, M. Landslide hazard assessment using random subspace fuzzy rules based classifier ensemble and probability analysis of rainfall data: A case study at mu cang chai district, yen bai province (Vietnam). *J. Indian Soc. Remote Sens.* **2017**, *45*, 673–683. [CrossRef]

27. Pham, B.T.; Prakash, I. Evaluation and comparison of logitboost ensemble, fisher's linear discriminant analysis, logistic regression and support vector machines methods for landslide susceptibility mapping. *Geocarto Int.* **2017**, *34*, 316–333. [CrossRef]

28. Pham, B.T.; Shirzadi, A.; Bui, D.T.; Prakash, I.; Dholakia, M. A hybrid machine learning ensemble approach based on a radial basis function neural network and rotation forest for landslide susceptibility modeling: A case study in the himalayan area, india. *Int. J. Sediment Res.* **2018**, *33*, 157–170. [CrossRef]

29. Pham, B.T.; Prakash, I. Machine learning methods of kernel logistic regression and classification and regression trees for landslide susceptibility assessment at part of himalayan area, India. *Indian J. Sci. Technol.* **2018**, *11*, 1–11. [CrossRef]

30. Ripley, B.D. *Pattern Recognition and Neural Networks*; Cambridge University Press: Cambridge, UK, 1996; pp. 1–403.

31. Adeli, H. Neural networks in civil engineering: 1989–2000. *Comput. Aided Civ. Infrastruct. Eng.* **2001**, *16*, 126–142. [CrossRef]

32. Rutherford, K.L.; Hatto, P.W.; Davis, C.; Hutchings, I.M. Abrasive wear resistance of TiN/NbN multi-layers: Measurement and neural network modelling. *Surf. Coat. Technol.* **1996**, *86*, 472–479. [CrossRef]

33. Jones, S.P.; Jansen, R.; Fusaro, R.L. Preliminary investigation of neural network techniques to predict tribological properties. *Tribol. Trans.* **1997**, *40*, 312–320. [CrossRef]

34. Ramesh, R.; Gnanamoorthy, R. Artificial neural network prediction of fretting wear behavior of structural steel, En 24 against bearing steel, En 31. *J. Mater. Eng. Perform.* **2007**, *16*, 703–709. [CrossRef]

35. Srinivasan, V.; Maheshkumar, K.V.; Karthikeyan, R.; Palanikumar, K. Application of probablistic neural network for the development of wear mechanism map for glass fiber reinforced plastics. *J. Reinf. Plast. Compos.* **2007**, *26*, 1893–1906. [CrossRef]

36. Hayajneh, M.; Hassan, A.M.; Alrashdan, A.; Mayyas, A.T. Prediction of tribological behavior of aluminum–copper based composite using artificial neural network. *J. Alloys Compd.* **2009**, *470*, 584–588. [CrossRef]

37. Rashed, F.S.; Mahmoud, T.S. Prediction of wear behaviour of A356/SiCp MMCs using neural networks. *Tribol. Int.* **2009**, *42*, 642–648. [CrossRef]

38. Shabani, M.O.; Mazahery, A. Modeling of the wear behavior in A356–B4C composites. *J. Mater. Sci.* **2011**, *46*, 6700–6708. [CrossRef]

39. Abdelbary, A.; Abouelwafa, M.N.; El Fahham, I.M.; Hamdy, A.H. Modeling the wear of Polyamide 66 using artificial neural network. *Mater. Des.* **2012**, *41*, 460–469. [CrossRef]

40. Stojanovic, B.; Blagojevic, J.; Babic, M.; Velickovic, S.; Miladinovic, S. Optimization of hybrid aluminum composites wear using Taguchi method and artificial neural network. *Ind. Lubr. Tribol.* **2017**, *69*, 1005–1015. [CrossRef]

41. Pillai, N.; Karthikeyan, R.; Davim, J.P. Heat treatment effects on tribological characteristics for AISI A8 tool steel and development of wear mechanism maps using K means clustering and neural networks. *Tribol. Mater. Surf. Interfaces* **2018**, *12*, 44–56. [CrossRef]

42. Zain, A.M.; Haron, H.; Sharif, S. Prediction of surface roughness in the end milling machining using artificial neural network. *Expert Syst. Appl.* **2010**, *37*, 1755–1768. [CrossRef]

43. Malinov, S.; Sha, W. Application of artificial neural networks for modelling correlations in titanium alloys. *Mater. Sci. Eng. A* **2004**, *365*, 202–211. [CrossRef]

44. Bhadeshia, H.K.D.H.; Dimitriu, R.C.; Forsik, S.; Pak, J.H.; Ryu, J.H. Performance of neural networks in materials science. *Mater. Sci. Technol.* **2009**, *25*, 504–510. [CrossRef]

45. Dixit, U.S.; Joshi, S.N.; Davim, J.P. Incorporation of material behavior in modeling of metal forming and machining processes: A review. *Mater. Des.* **2011**, *32*, 3655–3670. [CrossRef]

46. Stojanović, B.; Vencl, A.; Bobić, I.; Miladinović, S.; Skerlić, J. Experimental optimisation of the tribological behaviour of Al/SiC/Gr hybrid composites based on Taguchi's method and artificial neural network. *J. Braz. Soc. Mech. Sci. Eng.* **2018**, *40*, 311. [CrossRef]

47. Veličković, S.; Stojanović, B.; Babić, M.; Vencl, A.; Bobić, I.; Bognár, G.V.; Vučetić, F. Parametric optimization of the aluminium nanocomposites wear rate. *J. Braz. Soc. Mech. Sci. Eng.* **2019**, *41*, 19. [CrossRef]

48. Chen, S.L.; Wood, R.J.K.; Wang, L.; Callan, R.; Powrie, H.E.G. Wear detection of rolling element bearings using multiple-sensing technologies and mixture-model-based clustering method. *Proc. Inst. Mech. Eng. Part O J. Risk Reliab.* **2008**, *222*, 207–218.

49. Hornik, K.; Stinchcombe, M.; White, H. Multilayer feedforward networks are universal approximators. *Neural Netw.* **1989**, *2*, 359–366. [CrossRef]

50. Asteris, P.G.; Plevris, V. Neural network approximation of the masonry failure under biaxial compressive stress. In Proceedings of the 3rd South-East European Conference on Computational Mechanics—An ECCOMAS and IACM Special Interest Conference, Kos Island, Greece, 12–14 June 2013; Papadrakakis, M., Kojic, I., Tuncer, M., Eds.

51. Asteris, P.G.; Kolovos, K.G.; Douvika, M.G.; Roinos, K. Prediction of self-compacting concrete strength using artificial neural networks. *Eur. J. Environ. Civ. Eng.* **2016**, *20*, s102–s122. [CrossRef]

52. Asteris, P.G.; Tsaris, A.K.; Cavaleri, L.; Repapis, C.C.; Papalou, A.; Di Trapani, F.; Karypidis, D.F. Prediction of the fundamental period of infilled rc frame structures using artificial neural networks. *Comput. Intell. Neurosci.* **2016**, *2016*, 5104907. [CrossRef] [PubMed]

53. Asteris, P.G.; Roussis, P.C.; Douvika, M.G. Feed-forward neural network prediction of the mechanical properties of sandcrete materials. *Sensors* **2017**, *17*, 1344. [CrossRef] [PubMed]

54. Asteris, P.G.; Plevris, V. Anisotropic masonry failure criterion using artificial neural networks. *Neural Comput. Appl.* **2017**, *28*, 2207–2229. [CrossRef]

55. Asteris, P.G.; Kolovos, K.G. Self-compacting concrete strength prediction using surrogate models. *Neural Comput. Appl.* **2018**, *31*, 409–424. [CrossRef]

56. Cavaleri, L.; Chatzarakis, G.E.; Di Trapani, F.; Douvika, M.G.; Foskolos, F.M.; Fotos, A.; Giovanis, D.G.; Karypidis, D.F.; Livieratos, S.; Roinos, K.; et al. Surface roughness prediction of electro-discharge machined components using artificial neural networks. In Proceedings of the 5th International Conference on Integrity, Reliability and Failure, Faculty of Engineering/U, Porto, Portugal, 24–28 July 2016.

57. Cavaleri, L.; Chatzarakis, G.E.; Di Trapani, F.; Douvika, M.G.; Roinos, K.; Vaxevanidis, N.M.; Asteris, P.G. Modeling of surface roughness in electro-discharge machining using artificial neural networks. *Adv. Mater. Res.* **2017**, *6*, 169–184.

58. Bartlett, P.L. The sample complexity of pattern classification with neural networks: The size of the weights is more important than the size of the network. *IEEE Transact. Inf. Theory* **1998**, *44*, 525–536. [CrossRef]

59. Karlik, B.; Olgac, A.V. Performance analysis of various activation functions in generalized MLP architectures of neural networks. *Int. J. Artif. Intell. Expert Syst.* **2011**, *1*, 111–122.

60. Psyllaki, P.; Stamatiou, K.; Iliadis, I.; Mourlas, A.; Asteris, P.; Vaxevanidis, N. Surface treatment of tool steels against galling failure. In *MATEC Web of Conferences*; EDP Sciences: Les Ulis, France, 2018; Volume 188, p. 4024.

61. Lourakis, M.I.A. *A Brief Description of the Levenberg-Marquardt Algorithm Implemened by Levmar*; Hellas (FORTH) Institute of Computer Science Foundation for Research and Technology: Heraklion, Greece, 2005; Available online: http://www.ics.forth.gr/~{}lourakis/levmar/levmar (accessed on 10 July 2019).

62. Delen, D.; Sharda, R.; Bessonov, M. Identifying significant predictors of injury severity in traffic accidents using a series of artificial neural networks. *Accid. Anal. Prev.* **2006**, *38*, 434–444. [CrossRef] [PubMed]

63. Iruansi, O.; Guadagnini, M.; Pilakoutas, K.; Neocleous, K. Predicting the shear strength of rc beams without stirrups using bayesian neural network. In Proceedings of the 4th International Workshop on Reliable Engineering Computing, Robust Design—Coping with Hazards, Risk and Uncertainty, Singapore, 3–5 March 2010.

64. Asteris, P.G.; Moropoulou, A.; Skentou, A.D.; Apostolopoulou, M.; Mohebkhah, A.; Cavaleri, L.; Rodrigues, H.; Varum, H. Stochastic vulnerability assessment of masonry structures: Concepts, modeling and restoration aspects. *Appl. Sci.* **2019**, *9*, 243. [CrossRef]

65. Asteris, P.G.; Nozhati, S.; Nikoo, M.; Cavaleri, L.; Nikoo, M. Krill herd algorithm-based neural network in structural seismic reliability evaluation. *Mech. Adv. Mater. Struct.* **2019**, *26*, 1146–1153. [CrossRef]

66. Chen, H.; Asteris, P.G.; Armaghani, D.J.; Gordan, B.; Pham, B.T. Assessing dynamic conditions of the retaining wall using two hybrid intelligent models. *Appl. Sci.* **2019**, *9*, 1042. [CrossRef]

67. Asteris, P.G.; Argyropoulos, I.; Cavaleri, L.; Rodrigues, H.; Varum, H.; Thomas, J.; Lourenço, P.B. Masonry compressive strength prediction using artificial neural networks. In Proceedings of the 1st International Conference TMM_CH, Transdisciplinary Multispectral Modelling and Cooperation for the Preservation of Cultural Heritage, Athens, Greece, 10–13 October 2018.

68. Mohamad, E.T.; Faradonbeh, R.S.; Armaghani, D.J.; Monjezi, M.; Majid, M.Z.A. An optimized ANN model based on genetic algorithm for predicting ripping production. *Neural Comput. Appl.* **2017**, *28*, 393–406. [CrossRef]

69. Asteris, P.G.; Nikoo, M. Artificial bee colony-based neural network for the prediction of the fundamental period of infilled frame structures. *Neural Comput. Appl.* **2019**. [CrossRef]

70. Apostolopoulou, M.; Douvika, M.G.; Kanellopoulos, I.N.; Moropoulou, A.; Asteris, P.G. Prediction of compressive strength of mortars using artificial neural networks. In Proceedings of the 1st International Conference TMM_CH, Transdisciplinary Multispectral Modelling and Cooperation for the Preservation of Cultural Heritage, Athens, Greece, 10–13 October 2018.

71. Nikoo, M.; Ramezani, F.; Hadzima-Nyarko, M.; Nyarko, E.K.; Nikoo, M. Flood-routing modeling with neural network optimized by social-based algorithm. *Nat. Hazards* **2016**, *82*, 1–24. [CrossRef]

72. Nikoo, M.; Sadowski, L.; Khademi, F.; Nikoo, M. Determination of damage in reinforced concrete frames with shear walls using self-organizing feature map. *Appl. Comput. Intell. Soft Comput.* **2017**, *2017*, 3508189. [CrossRef]

73. Nikoo, M.; Hadzima-Nyarko, M.; Nyarko, K.E.; Nikoo, M. Determining the natural frequency of cantilever beams using ann and heuristic search. *Appl. Artif. Intell.* **2018**, *32*, 309–334. [CrossRef]

74. Abad, S.V.A.N.K.; Yilmaz, M.; Armaghani, D.J.; Tugrul, A. Prediction of the durability of limestone aggregates using computational techniques. *Neural Comput. Appl.* **2018**, *29*, 423–433. [CrossRef]

75. Koopialipoor, M.; Armaghani, D.J.; Hedayat, A.; Marto, A.; Gordan, B. Applying various hybrid intelligent systems to evaluate and predict slope stability under static and dynamic conditions. *Soft Comput.* **2018**, *23*, 5913–5929. [CrossRef]

76. Pham, B.T.; Khosravi, K.; Prakash, I. Application and comparison of decision tree-based machine learning methods in landside susceptibility assessment at Pauri Garhwal area, Uttarakhand, India. *Environ. Process.* **2017**, *4*, 711–730. [CrossRef]

77. Pham, B.T.; Bui, D.T.; Prakash, I.; Nguyen, L.H.; Dholakia, M. A comparative study of sequential minimal optimization-based support vector machines, vote feature intervals, and logistic regression in landslide susceptibility assessment using gis. *Environ. Earth Sci.* **2017**, *76*, 371. [CrossRef]

78. Ly, H.-B.; Le, L.M.; Duong, H.T.; Nguyen, T.C.; Pham, T.A.; Le, T.-T.; Le, V.M.; Nguyen-Ngoc, L.; Pham, B.T. Hybrid artificial intelligence approaches for predicting critical buckling load of structural members under compression considering the influence of initial geometric imperfections. *Appl. Sci.* **2019**, *9*, 2258. [CrossRef]

79. Koopialipoor, M.; Fahimifar, A.; Ghaleini, E.N.; Momenzadeh, M.; Armaghani, D.J. Development of a new hybrid ANN for solving a geotechnical problem related to tunnel boring machine performance. *Eng. Comput.* **2019**. [CrossRef]

80. Koopialipoor, M.; Ghaleini, E.N.; Tootoonchi, H.; Armaghani, D.J.; Haghighi, M.; Hedayat, A. Developing a new intelligent technique to predict overbreak in tunnels using an artificial bee colony-based ANN. *Environ. Earth Sci.* **2019**, *78*, 165. [CrossRef]

81. Gordan, B.; Jahed Armaghani, D.; Hajihassani, M.; Monjezi, M. Prediction of seismic slope stability through combination of particle swarm optimization and neural network. *Eng. Comput.* **2015**, *32*, 85–97. [CrossRef]

82. Hasanipanah, M.; Armaghani, D.J.; Amnieh, H.B.; Koopialipoor, M.; Arab, H. A risk-based technique to analyzeflyrock results through rock engineering system. *Geotech. Geol. Eng.* **2018**, *36*, 2247–2260. [CrossRef]

83. Koopialipoor, M.; Nikouei, S.S.; Marto, A.; Fahimifar, A.; Armaghani, D.J.; Mohamad, E.T. Predicting tunnel boring machine performance through a new model based on the group method of data handling. *Bull. Eng. Geol. Environ.* **2018**, *78*, 3799–3813. [CrossRef]

84. Liao, X.; Khandelwal, M.; Yang, H.; Koopialipoor, M.; Murlidhar, B.R. Effects of a proper feature selection on prediction and optimization of drilling rate using intelligent techniques. *Eng. Comput.* **2019**. [CrossRef]

85. Gordan, B.; Koopialipoor, M.; Clementking, A.; Tootoonchi, H.; Mohamad, E.T. Estimating and optimizing safety factors of retaining wall through neural network and bee colony techniques. *Eng. Comput.* **2019**, *35*, 945–954. [CrossRef]

86. Zhao, Y.; Noorbakhsh, A.; Koopialipoor, M.; Azizi, A.; Tahir, M.M. A new methodology for optimization and prediction of rate of penetration during drilling operations. *Eng. Comput.* **2019**. [CrossRef]

87. Sarir, P.; Chen, J.; Asteris, P.G.; Armaghani, D.J.; Tahir, M.M. Developing GEP tree-based, neuro-swarm, and whale optimization models for evaluation of bearing capacity of concrete-filled steel tube columns. *Eng. Comput.* **2019**. [CrossRef]